Nano Research
DOI 10.1007/s12274-013-0351-5
Research Article
ISSN 1998-0124
CN 11-5974/O4

Evidence for structural phase transitions and large effective band gaps in quasi-metallic ultra-clean suspended carbon nanotubes

Shun-Wen Chang[1] (✉), Rohan Dhall[2], Moh Amer[2], Kentaro Sato[4], Riichiro Saito[4], and Stephen Cronin[1,2,3]

[1] *Department of Physics and Astronomy, University of Southern California, Los Angeles, CA 90089, USA*
[2] *Department of Electrical Engineering, University of Southern California, Los Angeles, CA 90089, USA*
[3] *Department of Chemistry, University of Southern California, Los Angeles, CA 90089, USA*
[4] *Department of Physics, Tohoku University, Sendai 980-8578, Japan*

Received: 7 June 2013
Revised: 17 July 2013
Accepted: 17 July 2013

KEYWORDS
carbon nanotube,
Raman spectroscopy,
phase transition,
bandgap energy

ABSTRACT

We report evidence for a structural phase transition in individual suspended metallic carbon nanotubes by examining their Raman spectra and electron transport under electrostatic gate potentials. The current–gate voltage characteristics reveal anomalously large quasi-metallic band gaps as high as 240 meV, the largest reported to date. For nanotubes with band gaps larger than 200 meV, we observe a pronounced M-shape profile in the gate dependence of the 2D band (or G′ band) Raman frequency. The pronounced dip (or softening) of the phonon mode near zero gate voltage can be attributed to a structural phase transition (SPT) that occurs at the charge neutrality point (CNP). The 2D band Raman intensity also changes abruptly near the CNP, providing further evidence for a change in the lattice symmetry and a possible SPT. Pronounced non-adiabatic effects are observed in the gate dependence of the G band Raman mode, however, this behavior deviates from non-adiabatic theory near the CNP. For nanotubes with band gaps larger than 200 meV, non-adiabatic effects should be largely suppressed, which is not observed experimentally. This data suggests that these large effective band gaps are primarily caused by a SPT to an insulating state, which causes the large modulation observed in the conductance around the CNP. Possible mechanisms for this SPT are discussed, including electron–electron (e.g., Mott) and electron–phonon (e.g., Peierls) driven transitions.

The ability to grow ultra-clean, nearly defect free, suspended carbon nanotube field-effect transistors was first developed by Cao et al. in 2005 [1]. Since then, several interesting phenomena have been observed in these pristine, unperturbed nanotubes, including non-equilibrium phonon populations [2], pronounced Kohn

Address correspondence to Shunwenc@usc.edu

anomalies due to strong electron–phonon interactions [3], non-adiabatic effects and breakdown of the Born–Oppenheimer approximation [4], Wigner crystallization [5], and possible Mott insulator behavior due to strong electron–electron interactions [6]. These phenomena are only seen in pristine unperturbed nanotubes, indicating how sensitive this one-dimensional material is to slight defects, surface contaminants, and substrate interactions [7]. For example, the observation of non-adiabatic effects (i.e., breakdown of the Born–Oppenheimer approximation) in carbon nanotubes was not a surprising finding, based on their long electron lifetimes and the short vibrational cycle of the tightly bound carbon atoms. However, this was not observed prior to 2009 in substrate-supported nanotubes [8–11]. Desphande et al. first pointed out that the quasi-metallic band gaps observed in these ultra-clean, nearly defect-free, suspended nanotubes were anomalously large, exceeding the band gaps predicted from curvature induced effects [6, 12]. In particular, they showed that metallic armchair nanotubes, which should have no curvature-induced band gap [12], had finite band gaps on the order of 10–100 meV. A Mott insulator transition was proposed as a possible explanation, in which the strong Coulomb repulsion at half filling of the energy bands localize electrons, one electron per atom site, to form a Mott insulator [13]. This typically results in slight changes in the lattice structure of the material. Raman intensity modulation has been reported previously for Mott insulator transitions in other materials systems, including $LaSrTiO_3$ and $YCaTiO_3$, due to a lowering of the crystal symmetry and an increase in the effective mass m^* associated with the Mott state [14]. Previous experiments with bulk Mott insulators used chemical impurity doping, which introduces additional disorder into the system. Carbon nanotubes, however, offer the opportunity to study electronic phenomena without interference from disorder by electrostatic doping. A Peierls distortion would also produce a band gap in this system, but has only been predicted theoretically in nanotubes with very small diameters (~0.5 nm) and at very low temperatures, and is not expected to occur in the relatively large diameter nanotubes grown in this study.

Previous Raman studies of ultra-clean, nearly defect-free, suspended carbon nanotubes focused primarily on the *G* band Raman mode [2, 4, 15]. In this paper, we present the electrostatic doping dependence of the 2D band (also known as G′ band) Raman mode, which is not significantly affected by the Kohn anomaly or non-adiabatic effects in the nanotube and, thus, provides a more direct means for observing changes in the lattice structure and bond strengths of the nanotube. The effects observed in the Raman spectra are correlated with I–V_{gate} transport data, which exhibit large effective band gaps of ~200 meV.

Suspended carbon nanotubes (CNTs) were grown by chemical vapor deposition (CVD) on pre-patterned wafers using ferric nitrate catalyst at 825 °C. Before growth, platinum source and drain electrodes were patterned on a $Si/SiO_2/Si_3N_4$ wafer, together with a gate electrode in a 500 nm deep, 2 μm wide trench etched into the wafer [15]. The resulting field effect transistor (FET) device geometry is shown in Figs. 1(a) and 1(b). The nanotube growth is the final step in this sample fabrication process, which ensures that these nanotubes are not contaminated by any chemical residues from the lithographic fabrication processes.

The current–bias voltage (I–V_b) and conductance–gate voltage (G–V_g) characteristics of each device were

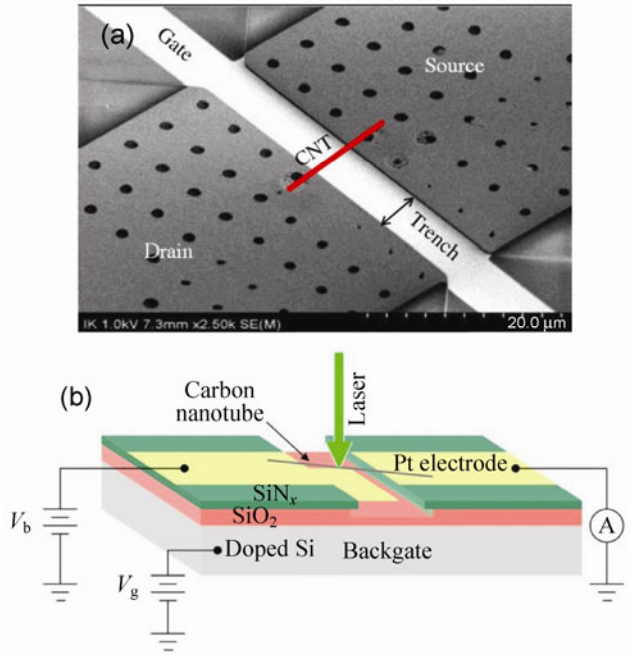

Figure 1 (a) Scanning electron microscope image and (b) schematic diagram of suspended carbon nanotube field effect transistor device.

recorded on a probe station, allowing us to separate metallic from semiconducting nanotube devices. High bias transport measurements were performed in an argon environment to determine whether the device is suspended, which is indicated by a region of negative differential conductance (NDC) [16]. The value of the maximum current enables us to determine if the device is a single isolated CNT or a bundle, as established by Pop et al. [16]. Single metallic CNTs that passed these selection criteria were selected and wire-bonded for further characterization. We then collected Raman spectra with either 633 nm or 532 nm wavelength radiation. The laser beam was focused to an approximately 1 μm spot size and attenuated by neutral density filters to ensure that heating was minimal, with a power of 20 μW. None of the devices reported here exhibited any detectible defect-induced D band Raman mode around 1,350 cm^{-1} [17].

Figure 2(a) shows the gate voltage dependence of the 2D Raman mode for a single suspended metallic carbon nanotube measured at room temperature, exhibiting a clear "M" shape profile. This "M" shape profile has a linear background with a slope of approximately –0.33 $cm^{-1}·V^{-1}$, which can be attributed to doping-induced weakening of the carbon–carbon bonds, and hence softening of the phonon modes. The dip occurring around zero gate voltage can be understood as the result of a structural phase transition (SPT) occurring at the charge neutrality point, causing a slight change in the lattice symmetry/bond strength, as discussed below.

Figure 2(b) shows the conductance–gate voltage characteristics for the same CNT shown in Fig. 2(a). This data was fitted using a Landauer transport model, giving an estimated band gap of the nanotube of 220 meV. Here, we also fitted the I–V_{gate} data using a Landauer model, as discussed previously [7, 18]. Briefly, the low bias conductance of the device can be expressed as

$$G = \left(\frac{4e^2}{h}\right)\int_{-\infty}^{\infty}\left(\frac{\lambda_{eff}}{\lambda_{eff}+L}\right)\left(\frac{-\partial f}{\partial E}\right)dE \quad (1)$$

where λ_{eff} is the effective mean free path (given by Matthiessen's rule), L is the device length, and $\frac{\partial f}{\partial E}$ is the derivative of the Fermi–Dirac distribution [19].

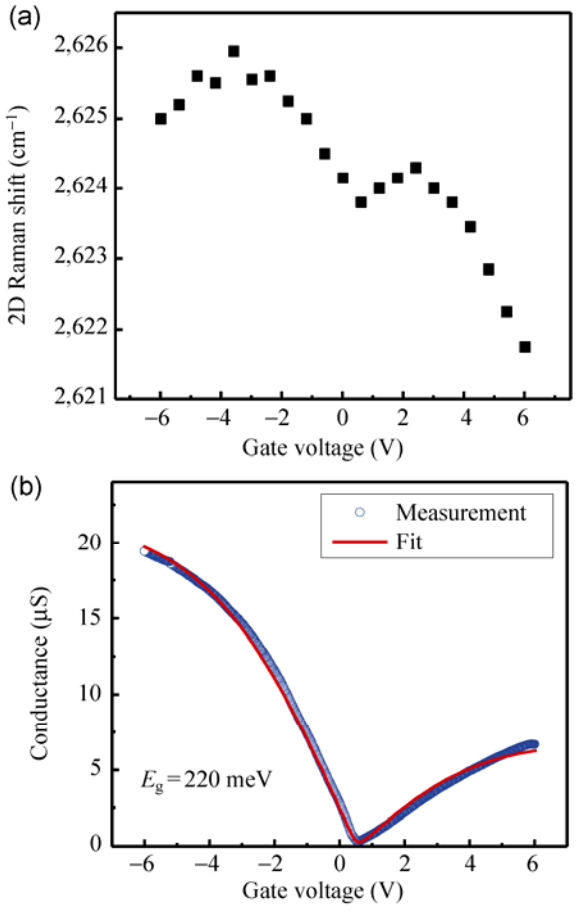

Figure 2 (a) Gate voltage dependence of the 2D band Raman shift and (b) conductance–gate voltage curve for a suspended metallic CNT measured at room temperature.

Using a hyperbolic energy dispersion relation, we integrate over the density of states which is given by

$$D(E) = \sum_{j=1}^{N}\left|\frac{dE_j(k)}{dk}\right|^{-1} \quad (2)$$

Here, the density of states is zero inside the band gap, E_g. The Fermi energy in the nanotube is related to the applied gate voltage according to the following relation [18, 20, 21]:

$$E_F + \frac{Q}{C} = eV_g \quad (3)$$

where E_F is the Fermi energy, Q is the electric charge on the nanotube, and C is the geometric capacitance. The electric charge is calculated by

$$Q = \int_{bands} D(E)f(E)dE \quad (4)$$

where $D(E)$ is the density of states, and $f(E)$ is the Fermi function.

Figure 3(a) shows the gate voltage dependence of the 2D band for another suspended quasi-metallic CNT device. Here, a slight monotonic decrease in the 2D band frequency is observed under applied gate voltages with a slope of approximately –0.25 $cm^{-1} \cdot V^{-1}$, consistent with doping-induced expansion of the carbon–carbon bond. A band gap of 56 meV was determined from a Landauer fit of the G–V_g data shown in Fig. 3(b). This behavior was observed consistently in four other nanotubes measured whose effective transport band gaps were below 100 meV.

As reported in our previous work, the gate dependence of the G band Raman mode exhibits a pronounced W-shape profile, as shown in Fig. 4(a), which arises from non-adiabatic behavior observed through the strong Kohn anomaly in the nanotube.

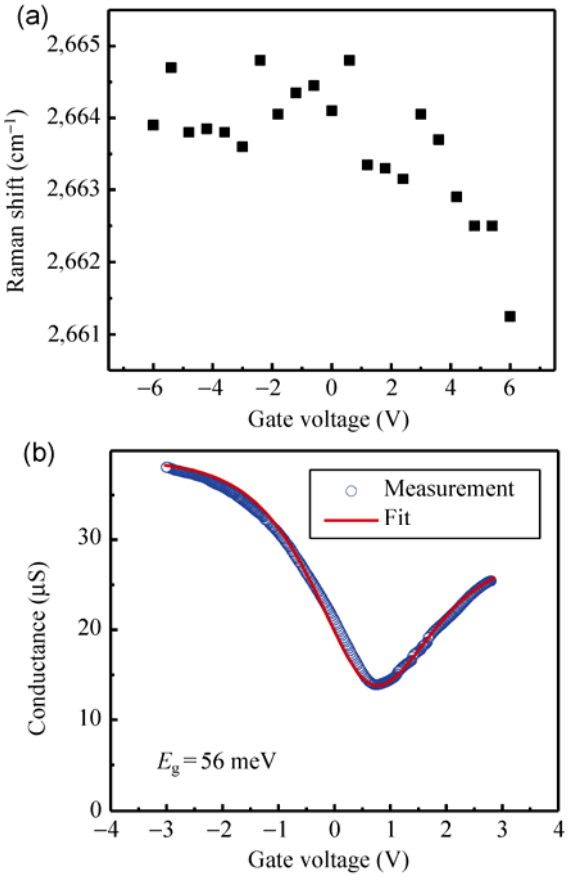

Figure 3 (a) Gate voltage dependence of the 2D band Raman shift and (b) conductance–gate voltage curve for another suspended quasi-metallic CNT measured at room temperature.

This W-shape profile was first predicted theoretically [10, 12, 22, 23] and later observed experimentally [3, 4]. Figure 4(b) shows the non-adiabatic doping dependence of the G band calculated at room temperature using second order perturbation theory for a quasi-metallic nanotube with various band gaps. Following the treatment of Sasaki et al. [12], we calculate the phonon self energy, $\Pi(\omega, E_F)$, using the expression in Eq. (5).

$$\Pi(\omega, E_F) = 2\Sigma_k \left(\frac{|V_k|^2}{\hbar\omega - E_k^{eh} + \frac{i\Gamma}{2}} - \frac{|V_k|^2}{\hbar\omega + E_k^{eh} + \frac{i\Gamma}{2}} \right) (f^h - f^e) \quad (5)$$

where V_k is the electron–phonon coupling matrix element, $\hbar\omega$ is the phonon energy (0.196 eV), $E^{eh} = E^e - E^h$ (where $E^{e(h)}$ is the electron (hole) state energy, given by the hyperbolic dispersion), $f^{e(h)}$ is the Fermi occupation function for electrons (holes), and Γ is determined self consistently from the imaginary part of the phonon self energy. The real part of the phonon self energy gives the renormalization of the phonon energy due to electron–phonon interaction.

Figure 4(b) shows the calculated relative Raman shift of the G band due to non-adiabatic phonon renormalization. Here, the W-shape profile becomes significantly weaker for a band gap of 100 meV, and is completely absent for a nanotubes with a band gap of 200 meV. That is, when the band gap of the nanotube is larger than the optical phonon energy (196 meV), the dominant contribution for perturbation ($E^{eh}=\hbar\omega$) is suppressed. Also, notice that the slope of the G band Raman shift with respect to gate voltage is non-zero in the experimental data near the charge neutrality point (CNP), whereas theory predicts a zero slope. This deviation from theory is observed consistently in all metallic nanotubes measured with large band gaps. The pronounced non-adiabatic W-shape profile observed experimentally indicates that the actual separation between the conduction and valence bands must be smaller than 200 meV. This suggests that the large effective band gaps observed in the I–V_g characteristics are primarily caused by a SPT to an insulating state, which causes a large modulation in the conductance around the CNP.

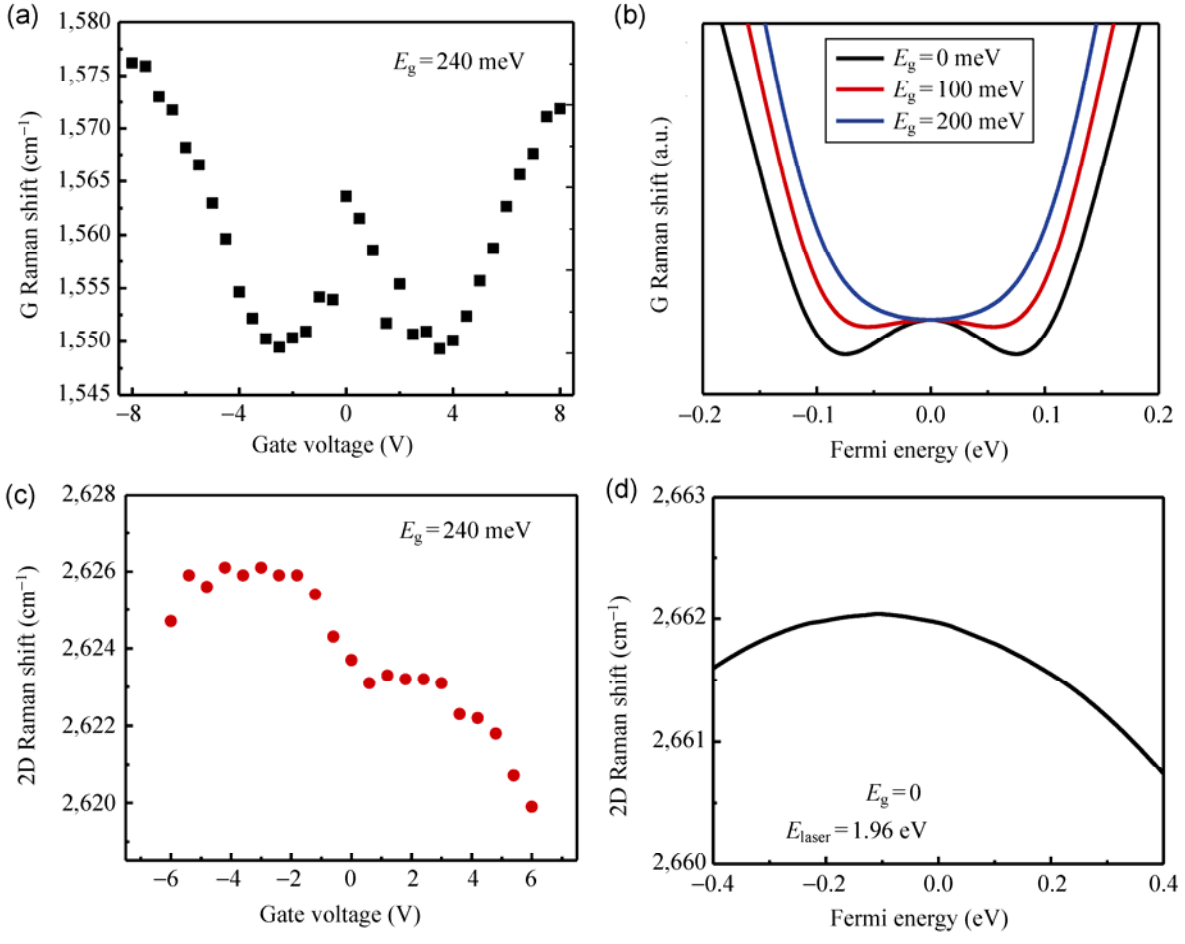

Figure 4 Experimentally measured (a) G and (c) 2D Raman modes taken from the same nanotube at room temperature. Non-adiabatic calculations of the gate dependence of the (b) G and (d) 2D bands.

Figure 4(c) shows the gate dependence of the 2D band, which also shows the same M-shape profile seen in Fig. 2(a). Near the CNP, the 2D band exhibits a monotonically decreasing gate dependence with a slope of approximately –0.5 cm^{-1}·V^{-1}. The 2D band Raman mode is affected much less by the Kohn anomaly than the G band and, thus, provides a more reliable means for observing changes in the lattice structure and bond strengths of the nanotube. Figure 4(d) shows the non-adiabatic doping dependence of the 2D Raman mode calculated using Eq. (5). Since the 2D band does not exhibit significant non-adiabatic effects, the M-shape profile shown in Fig. 4(c) indicates the existence of a different mechanism for phonon softening at the CNP. Araujo et al. observed an upside down V-shape gate dependence in the 2D band of single layer graphene [24]. This behavior was attributed to non-adiabatic effects; however, no rigorous calculations were given. In the 2D data shown in Figs. 2(a) and 4(c), the downturns at the two ends of the M-shape profile could be due to non-adiabatic effects, while the dip at the CNP is due to the SPT.

We also observe dramatic changes in the 2D band Raman intensity, as shown in Figs. 5(a) and 5(b). Our previous measurements of the G band Raman intensity have shown similar changes with doping [3, 15]. Typically, changes in the Raman intensity of CNTs are attributed to a change in the resonance condition (ΔE_{ii}). Such a large change in the Raman intensity (5X) would require a change in the resonant optical transition energy of $\Delta E_{ii} \geqslant 50$ meV. It is tempting to attribute the changes observed in Raman frequency and Raman intensity to strain induced by the electrostatic gate force. However, this can be ruled out for several

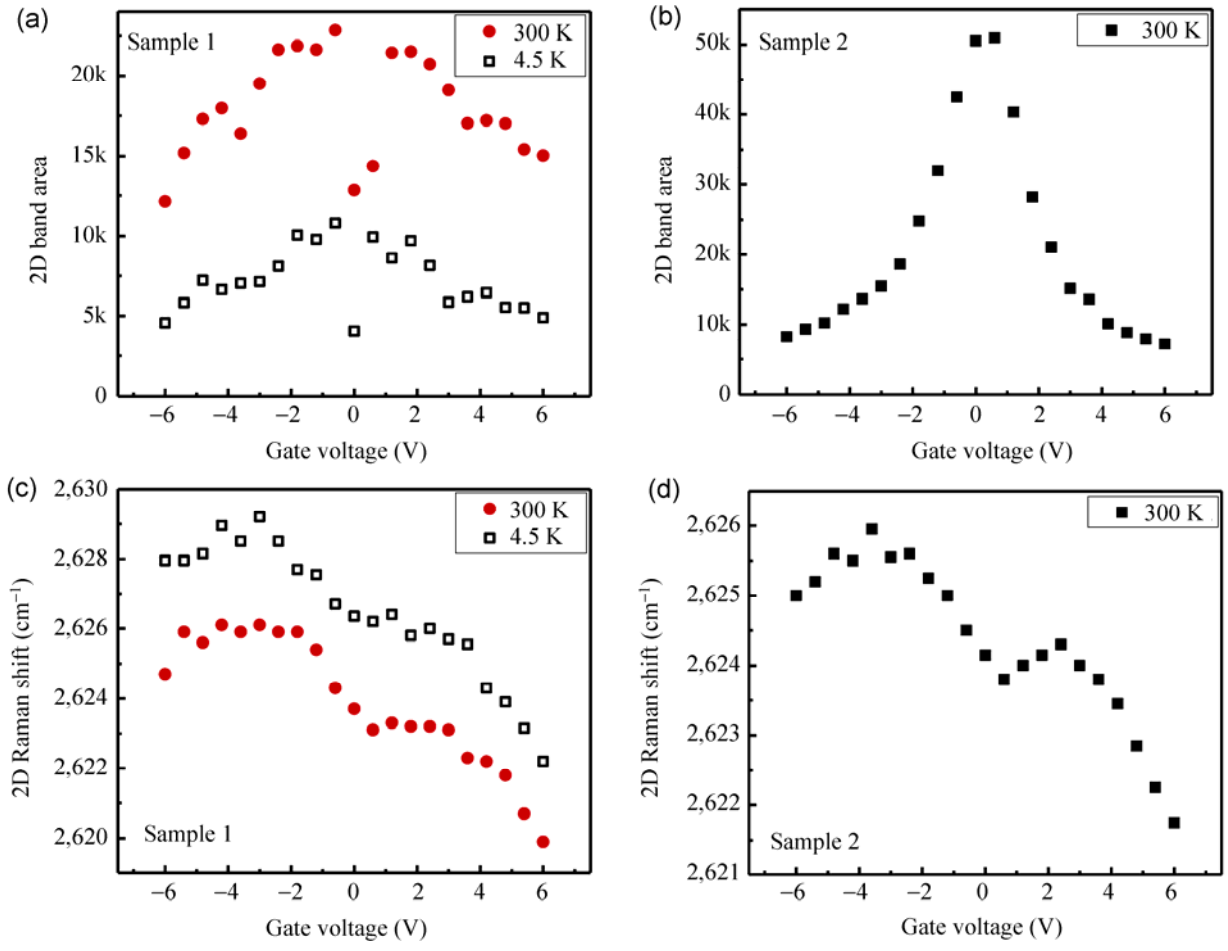

Figure 5 (a), (b) 2D band Raman integrated area intensities and (c), (d) Raman shifts for two different quasi-metallic devices (Sample 1 and Sample 2).

reasons. First, the nanotube will be pulled towards the bottom of the trench with a force given by $F = \frac{1}{2C'V_g^2}$, where $C' = dC/dz$ is the derivative of the capacitance with respect to the distance between the nanotube and the gate electrode. Assuming a Young's modulus of 1 TPa [25] and a strain-induced downshift rate of $dW_{G'}/d\sigma = -5.2\ cm^{-1}\cdot GPa^{-1}$ [26], a tension of 0.38 GPa would be required to produce the 2 cm^{-1} change in the Raman shift that is observed experimentally. This corresponds to an applied gate voltage of more than 40 V [27, 28], which is one order of magnitude higher than the actual gate voltage applied in this study, and thus negligible. Furthermore, any change in Raman shift due to gate voltage induced strain would produce a monotonically decreasing change, not an abrupt M-shaped change, where there is first a phonon hardening and then a softening. Second, we have not observed any changes in the radial breathing mode (RBM) anti-Stokes/Stokes intensity ratio, which is extremely sensitive even to small changes in the optical transition energies (i.e., E_{ii}) due to strain [15]. Lastly, no gate-induced changes in the Raman intensity or Raman frequency have ever been observed for suspended semiconducting nanotubes, further indicating that the phenomena observed here are not due to electromechanical forces. Here, we believe that a SPT occurring near the CNP results in significant changes in the matrix elements associated with the Raman process. The exact nature of this SPT, however, is still unknown and will require further studies. As a comparison, the CNT shown in Fig. 3 (E_g = 56 meV) showed no gate dependence of the Raman intensity.

Several possible mechanisms have been proposed to explain the band gaps observed in metallic carbon nanotubes. Early scanning tunneling microscopy (STM) studies of metallic nanotubes attributed these small energy gaps to the curvature of the nanotube [29]. The curvature-induced band gaps are given by $E_{gap} = C\cos(3\theta)/d_t^2$, where C is 60 meV·nm^2, d_t is the nanotube diameter, and θ is the chiral angle [12, 30]. For the range of diameters in this work, we expect band gaps of $E_{gap} \approx 0$–50 meV, which is more than four times smaller than the band gaps we observe. Armchair nanotubes, which theoretically should have $E_{gap} = 0$, have also been shown to exhibit substantial band gaps experimentally [6]. Like curvature, uniaxial strain can also result in a band gap [31, 32]; however, these types of symmetry-breaking band gaps can be closed with the application of an axial magnetic field, which was not observed experimentally in suspended CNTs [6], indicating that another underlying mechanism must be responsible for the observed band gaps. As mentioned above, the relatively large band gaps observed in ultra-clean, suspended quasi-metallic carbon nanotubes have been attributed to a Mott insulator transition arising from strong electron–electron interactions [6]. However, this mechanism has not been verified, and the exact nature of the Mott state is not known, including whether it exhibits a charge density wave, spin density wave, or otherwise [33, 34]. Many authors have calculated a Peierls instability in nanotubes, as early as 1992, predicting that this transition is unlikely because of the energy subband structure [23, 35–38]. Both a Peierls distortion and a Mott transition would result in a large modulation of the Raman intensity through a lowering of the crystal symmetry and an increase in the effective mass m^*. However, Peierls distortions have been predicted theoretically only in nanotubes with very small diameters (~0.5 nm) and are not expected to occur in the relatively large diameter nanotubes grown in this study. Both transitions are extremely sensitive to slight changes in the free charge density in the system [39, 40]. A change in the lattice constants and optical transition energies with Fermi energy have been predicted by first principles calculations in metallic nanotubes near the first pair of van Hove singularities [41]. Structural stabilization by a naturally occurring torsion of the nanotube has also been predicted to produce a band gap in metallic nanotubes [42]. Future studies are needed in order to establish the precise mechanism underlying the structural phase transition reported in this letter. It is likely that this modulation has not been observed until now because most previous studies of electrostatically gated carbon nanotubes were performed on nanotube-on-substrate devices rather than pristine, suspended devices. The Mott insulating state (and Peierls distortion) requires the presence of a well-defined charge neutrality point [20], which may not occur in samples with defects, substrate contact, or post-processing residue.

In conclusion, the electrostatic doping dependence of the Raman spectra and electron transport in ultra-clean suspended carbon nanotubes shows evidence for a structural phase transition. Near the charge neutrality point (CNP), effective band gaps as large as 240 meV are observed in the current–gate voltage characteristics of quasi-metallic nanotubes. A pronounced dip in the 2D band is also observed at the CNP indicating a change in the lattice or electronic structure. The measured gate dependence of the G and 2D band Raman shifts and intensities deviate from non-adiabatic calculations near the CNP, indicating the existence of another mechanism affecting the phonon modes. For nanotubes with smaller quasi-metallic band gaps (~50 meV), these Raman features are not observed near the charge neutrality point, indicating that the Raman and transport phenomena are related.

Acknowledgements

This work was supported in part by Department of Energy (Award No. DE-FG02-07ER46376 (SWC)) and Office of Naval Research (Award No. N000141010511) (RD) of the united states. A portion of this work was carried out in the University of California Santa Barbara (UCSB) nanofabrication facility, part of the National Science Foundation (NSF) funded National Nanotechnology Infrastructure Network (NNIN) network. This work was also supported in part by JSPS KAKENHI (Grant Nos. 20241023 and 23710118).

References

[1] Cao, J. E.; Wang, Q.; Dai, H. J. Electron transport in very clean, as-grown suspended carbon nanotubes. *Nat. Mater.*

2005, *4*, 745–749.

[2] Bushmaker, A. W.; Deshpande, V. V.; Bockrath, M. W.; Cronin, S. B. Direct observation of mode selective electron−phonon coupling in suspended carbon nanotubes. *Nano Lett.* **2007**, *7*, 3618–3622.

[3] Dhall, R.; Chang, S.-W.; Liu, Z. W.; Cronin, S. B. Pronounced electron-phonon interactions in ultraclean suspended carbon nanotubes. *Phys. Rev. B* **2012**, *86*, 045427.

[4] Bushmaker, A. W.; Deshpande, V. V.; Hsieh, S.; Bockrath, M. W.; Cronin, S. B. Direct observation of Born-Oppenheimer approximation breakdown in carbon nanotubes. *Nano Lett.* **2009**. *9*, 607–611.

[5] Deshpande, V. V.; Bockrath, M. The one-dimensional Wigner crystal in carbon nanotubes. *Nat. Phys.* **2008**, *4*, 314–318.

[6] Deshpande, V. V.; Chandra, B.; Caldwell, R.; Novikov, D. S.; Hone, J.; Bockrath, M. Mott insulating state in ultraclean carbon nanotubes. *Science* **2009**, 323, 106–110.

[7] Amer, M. R.; Bushmaker, A.; Cronin, S. B. The influence of substrate in determining the band gap of metallic carbon nanotubes. *Nano Lett.* **2012**, *12*, 4843–4847.

[8] Cronin, S. B.; Barnett, R.; Tinkham, M.; Chou, S. G.; Rabin, O.; Dresselhaus, M. S.; Swan, A. K.; Ünlü, M. S.; Goldberg, B. B. Electrochemical gating of individual single-wall carbon nanotubes observed by electron transport measurements and resonant Raman spectroscopy. *Appl. Phys. Lett.* **2004**, *84*, 2052–2054.

[9] Das, A.; Sood, A. K.; Govindaraj, A.; Marco Saitta, A.; Lazzeri, M.; Mauri, F.; Rao, C. N. R. Doping in carbon nanotubes probed by Raman and transport measurements. *Phys. Rev. Lett.* **2007**, *99*, 136803.

[10] Tsang, J. C.; Freitag, M.; Perebeinos, V.; Liu, J.; Avouris, P. Doping and phonon renormalization in carbon nanotubes. *Nat. Nanotechnol.* **2007**, *2*, 725–730.

[11] Farhat, H.; Son, H.; Samsonidze, G. G.; Reich, S.; Dresselhaus, M. S.; Kong, J. Phonon softening in individual metallic carbon nanotubes due to the Kohn anomaly. *Phys. Rev. Lett.* **2007**, *99*, 145506.

[12] Sasaki, K.; Farhat, H.; Saito, R.; Dresselhaus, M. S. Kohn anomaly in Raman spectroscopy of single wall carbon nanotubes. *Physica E* **2010**, *42*, 2005–2015.

[13] Mott, N. F. Metal-insulator transition. *Rev. Mod. Phys.* 1968, *40,* 677–683.

[14] Katsufuji, T.; Tokura, Y. Anomalous variation of phonon Raman intensities near the metal-to-Mott-insulator transition in titanium-oxide systems. *Phys. Rev. B* **1994**, *50*, 2704–2707.

[15] Bushmaker, A. W.; Deshpande, V. V.; Hsieh, S.; Bockrath, M. W.; Cronin, S. B. Large modulations in the intensity of Raman-scattered light from pristine carbon nanotubes. *Phys. Rev. Lett.* **2009**, *103*, 067401.

[16] Pop, E.; Mann, D.; Cao, J. E.; Wang, Q.; Goodson, K.; Dai, H. J. Negative differential conductance and hot phonons in suspended nanotube molecular wires. *Phys. Rev. Lett.* **2005**, *95*, 155505.

[17] Jorio, A.; Pimenta, M.; Souza Filho, A.; Saito, R.; Dresselhaus, G.; Dresselhaus, M. Characterizing carbon nanotube samples with resonance Raman scattering. *New J. Phys.* **2003**, *5,* 139.

[18] Bushmaker, A. W.; Deshpande, V. V.; Hsieh, S.; Bockrath, M. W.; Cronin, S. B. Gate voltage controllable non-equilibrium and non-ohmic behavior in suspended carbon nanotubes. *Nano Lett.* **2009**, *9*, 2862–2866.

[19] Zhao, Y.; Liao, A.; Pop, E. Multiband mobility in semiconducting carbon nanotubes. IEEE Electr. Device L. IEEE **2009**, *30*, 1078–1080.

[20] Bushmaker, A.; Chang, C.; Deshpande, V.; Amer, M.; Bockrath, M.; Cronin, S. Memristive behavior observed in a defected single-walled carbon nanotube. *IEEE T. Nanotechnol.* **2011**, 10, 582–586.

[21] Das, A.; Pisana, S.; Chakraborty, B.; Piscanec, S.; Saha, S. K.; Waghmare, U. V.; Novoselov, K. S.; Krishnamurthy, H. R.; Geim, A. K.; Ferrari, A. C.; et al. Monitoring dopants by Raman scattering in an electrochemically top-gated graphene transistor. *Nat. Nanotechnol.* **2008**, *3*, 210–215.

[22] Caudal, N.; Saitta, A. M.; Lazzeri, M.; Mauri, F. Kohn anomalies and nonadiabaticity in doped carbon nanotubes. *Phys. Rev. B* **2007**, *75*, 115423.

[23] Piscanec, S.; Lazzeri, M.; Robertson, J.; Ferrari, A. C.; Mauri, F. Optical phonons in carbon nanotubes: Kohn anomalies, Peierls distortions, and dynamic effects. *Phys. Rev. B* 2007, *75*, 035427.

[24] Araujo, P. T.; Mafra, D. L.; Sato, K.; Saito, R.; Kong, J.; Dresselhaus, M. S. Phonon self-energy corrections to nonzero wave-vector phonon modes in single-layer craphene. *Phys. Rev. Lett.* **2012**, ***109***, 046801.

[25] Wu, Y.; Huang, M. Y.; Wang, F.; Huang, X. M. H.; Rosenblatt, S.; Huang, L. M.; Yan, H. G.; O'Brien, S. P.; Hone, J.; Heinz, T. F. Determination of the Young's modulus of structurally defined carbon nanotubes. *Nano Lett.* **2008**, *8*, 4158–4161.

[26] Cronin, S. B.; Swan, A. K.; Ünlü, M. S.; Goldberg, B. B.; Dresselhaus, M. S.; Tinkham, M. Measuring the uniaxial strain of individual single-wall carbon nanotubes: Resonance Raman spectra of atomic-force-microscope modified single-wall nanotubes. *Phys. Rev. Lett.* **2004**, *93*, 167401.

[27] Cronin, S. B.; Swan, A. K.; Ünlü, M. S.; Goldberg, B. B.; Dresselhaus, M. S.; Tinkham, M. Measuring the uniaxial strain of individual single-wall carbon nanotubes: Resonance Raman spectra of atomic-force-microscope modified single-wall nanotubes. *Phys. Rev. Lett.* **2004**, *93*, 167401.

[28] Sapmaz, S.; Blanter, Y. M.; Gurevich, L.; Van der Zant, H.

S. J. Carbon nanotubes as nanoelectromechanical systems. *Phys. Rev. B* **2003**, *67*, 235414.

[29] Ouyang, M.; Huang, J.-L.; Cheung, C. L.; Lieber, C. M. Energy gaps in "metallic" single-walled carbon nanotubes. *Science* 2001, *292*, 702–705.

[30] Kane, C. L.; Mele, E. J. Size, shape, and low energy electronic structure of carbon nanotubes. *Phys. Rev. Lett.* **1997**, *78*, 1932–1935.

[31] Cronin, S. B.; Swan, A. K.; Ünlü, M. S.; Goldberg, B. B.; Dresselhaus, M. S.; Tinkham, M. Resonant Raman spectroscopy of individual metallic and semiconducting single-wall carbon nanotubes under uniaxial strain. *Phys. Rev. B* **2005**, *72*, 035425.

[32] Yang, L.; Anantram, M. P.; Han, J.; Lu, J. P. Band-gap change of carbon nanotubes: Effect of small uniaxial and torsional strain. *Phys. Rev. B* **1999**, *60*, 13874–13878.

[33] Balents, L.; Fisher, M. P. A. Correlation effects in carbon nanotubes. *Phys. Rev. B* **1997**, *55*, R11973–R11976.

[34] Krotov, Y. A.; Lee, D.-H.; Louie, S. G. Low energy properties of (n, n) carbon nanotubes. *Phys. Rev. Lett.* **1997**, *78*, 4245–4248.

[35] Barnett, R.; Demler, E.; Kaxiras, E. Electron-phonon interaction in ultrasmall-radius carbon nanotubes. *Phys. Rev. B* **2005**, *71*, 035429.

[36] Connetable, D.; Rignanese, G. M.; Charlier, J. C.; Blase, X. Room temperature Peierls distortion in small diameter nanotubes. *Phys. Rev. Lett.* **2005**, *94*, 015503.

[37] Dumont, G.; Boulanger, P.; Côté, M.; Ernzerhof, M. Peierls instability in carbon nanotubes: A first-principles study. *Phys. Rev. B* **2010**, *82*, 035419.

[38] Saito, R.; Fujita, M.; Dresselhaus, G.; Dresselhaus, M. S. Electronic-structure of graphene tubules based on C-60. *Phys. Rev. B* 1992, *46*, 1804–1811.

[39] Kim, H.-T.; Chae, B.-G.; Youn, D.-H.; Maeng, S.-L.; Kim, G.; Kang, K.-Y.; Lim, Y.-S. Mechanism and observation of Mott transition in VO_2-based two- and three-terminal devices. *New J. Phys*. **2004**, *6*, 52.

[40] Peierls, R. *More Surprises in Theoretical Physics*; Princeton University Press: Princeton, 1991.

[41] Yin, L.-C.; Cheng, H.-M.; Saito, R.; Dresselhaus, M. S. Fermi level dependent optical transition energy in metallic single-walled carbon nanotubes. *Carbon* **2011**, *49*, 4774–4780.

[42] Vercosa, D. G.; Barros, E. B.; Souza Filho, A. G.; Mendes Filho, J.; Samsonidze, G. G.; Saito, R.; Dresselhaus, M. S. Torsional instability of chiral carbon nanotubes. *Phys. Rev. B* 2010, *81*, 165430.